The Effect of Ship Speed, Heading Angle and Wave Steepness on the Likelihood of Broaching-To in Astern Quartering Seas

Pepijn de Jong, *Delft University of Technology*, pepijn.dejong@tudelft.nl

Martin. R. Renilson, *Higher Colleges of Technology, UAE, and Australian Maritime College,* martin@renilson-marine.com

Frans van Walree, *Maritime Research Institute Netherlands*, f.v.walree@marin.nl

ABSTRACT

A time domain simulation method that has been developed to investigate the non-linear behaviour of fast ships in waves is applied to following and astern quartering seas. The basis for the simulation method is a panel method employing linearization of some aspects of the hydrodynamics, combined with semi-empirical viscous models to enable faster computations and enabling a range of parameters to be studied in a realistic time frame.

This paper describes the application of the simulation method to the behaviour a fine form displacement hull shape in following and astern quartering seas. The effects of: vessel speed; wave length; heading angle to the waves; and wave steepness are investigated, and the implications on the likelihood of broaching-to in a realistic irregular seaway are inferred.

Keywords: *broaching-to, seakeeping and manoeuvring, time-domain panel method*

NOMENCLATURE

Roman

B	Beam	(m)
c	Wave celerity	(m/s)
Fr	Froude number	(-)
GM	Metacentric height	(m)
H	Wave height	(m)
L	Length	(m)
K,N	Manoeuvring moments	(Nm)
m	Ship mass	(kg)
r	Yaw rate	(rad/s)
R	Resistance	(N)
S	Wetted surface area	(m^2)
T	Draught	(m)
U	Forward speed	(m/s)
x,y,z	Spatial reference coordinates	(m)
X,Y,Z	Manoeuvring forces	(N)

Greek

β	Drift angle	(deg)
δ	Rudder deflection	(deg)
φ	Heel angle	(deg)
λ	Wave length	(m)
ρ	Density of sea water	(kg/m^3)
ξ	Long. position in the wave	(m)
ψ	Yaw (course deviation)	(deg)
ψ_w	Desired heading	(deg)
ζ	Wave elevation	(m)

An over-dot denotes a derivative with respect to time.

Non-dimensional parameters

$$Y' = \frac{Y}{½ \cdot \rho \cdot U^2 \cdot L^2} \qquad N' = \frac{N}{½ \cdot \rho \cdot U^2 \cdot L^3}$$

$$r' = \frac{r \cdot L}{U} \qquad v' = \frac{v}{U} \qquad m' = \frac{m}{½ \cdot \rho \cdot L^3}$$

1. INTRODUCTION

The control of vessels operating in severe following or astern quartering seas can be difficult, and in many cases can lead to broaching-to. Broaching occurs when a vessel is forced to yaw, and turns away from the wave direction, and towards a direction parallel to the waves. Often, the yaw is particularly violent, which, when combined with the rolling moment due to the counter rudder, and the wave induced rolling moment, can result in a sudden capsize (du Cane and Goodrich, 1962 and Renilson, 1980).

A time domain simulation model, termed PANSHIP, has been developed to investigate the broaching of a fast rescue craft (de Jong *et al.*, 2013). The results from this work showed that the method was able to predict the tendency of this vessel to broach in regular waves of varying length and steepness over range of forward speeds.

The current paper describes the application of the simulation model to investigate the broaching of a high speed fine form displacement vessel. In particular the influence of: ship speed; heading angle to the waves; wave length; and wave steepness have been investigated.

2. SIMULATION MODEL

The simulation of broaching in stern to stern-quartering waves is more complex than simulating ship motions in head to beam seas. One of the main difficulties is that in stern to stern-quartering seas a vessel's speed is likely to vary substantially due to the large longitudinal wave force, and the low encounter frequency. As the ship's hydrodynamic characteristics are functions of its longitudinal position in the wave, it is not normally possible to assume an "average" value, as is the usual practice in head seas. Thus, the situation is complicated by a substantial non-linearity, which must be taken into account carefully. This is unlike the behaviour in head seas, where to a large extent it is enough to consider the average position of the vessel in the wave.

On the other hand, as the encounter frequency is low it is often possible to assume quasi-steadiness, which can considerably simplify the situation. This low encounter frequency has inspired some authors to deal with surf-riding and broaching problems in a quasi-steady fashion, see for instance Renilson and Driscoll (1982). As a result of these low encounter frequencies potential flow damping is only slight and viscous forces due to friction and flow separation are important.

As the steepness of the waves increases, so does the tendency to broach, requiring simulation methods to deal with non-linear effects both in the waves and in the body motions. The resulting large variations in the instantaneous submerged body have an influence on the hydrostatic forces, the wave exciting forces, and the hydrodynamic disturbance forces. In extreme cases the large relative motions may lead to deck immersion, requiring incorporation of the dynamics of water on deck.

To completely deal with the above requires a fully non-linear simulation method, preferably including viscous flow effects. Up to now, these methods require a prohibitive amount of computational time and effort for a full time-domain simulation. Consequently, computational techniques, together with captive model experiments, are mostly used to derive manoeuvring coefficients for use in time domain simulations based on differential equations to simulate manoeuvring performance.

Here a time domain panel method is used, employing a linearization of part of the hydrodynamic problem combined with semi-empirical viscous models to enable faster computations and enabling full time domain simulation. This method, termed PANSHIP, is

described in detail in van Walree (2002) and de Jong (2011), and can be characterized by:

- Three-dimensional transient Green function to account for linearized free surface effects, exact forward speed effects, mean wetted surface, mean radiated and diffracted wave components along the hull and a Kutta condition at the stern;
- Three-dimensional panel method to account for Froude-Krylov forces on the instantaneous submerged body;
- Cross flow drag method for viscosity effects;
- Resistance obtained from pressure integration at each time step combined with empirical viscous drag;
- Propulsion using propeller open water characteristics or a semi-empirical water jet model;
- Motion control and steering using semi-empirical lifting-surface characteristics, water jet steering, and propeller-rudder interaction coefficients;
- Empirical viscous roll damping; and
- Autopilot steering and motion control.

The method has partly been developed and validated in the FAST2 and FAST3 research projects. The participants of these projects are Damen Shipyards (NL), Defence Science Technology Organisation (AUS), Royal Netherlands Navy (NL), Marin (NL) and Delft University of Technology (NL). The method has been validated using a range of physical model experiments, some of which are described in de Jong *et al.* (2013), including:

- Prediction of calm water running attitude and resistance;
- Steering moments from water jet propulsion; and
- Sway, yaw and roll manoeuvring forces/moments due to sway and yaw velocities.

3. APPLICATION

3.1 Fine form displacement vessel

The method was applied to the simulation of the motions of a fine form displacement vessel in following to quartering regular waves. This particular hull shape was used earlier in work published by Renilson and Driscoll (1982). They experimentally determined the manoeuvring coefficients for this hull form in slowly overtaking following and quartering regular waves. This was done by performing forced oscillations with the model mounted under a PMM in a circulating water channel outfitted with a wavedozer. The set of coefficients reported in that paper were used in this work to determine whether the current simulation model reflects a realistic manoeuvring behaviour for this type of vessel.

Figure 1 shows the body plan of the fine form displacement vessel and Table 1 presents the main particulars of the vessel. The hull lines were obtained by digitizing the body plan given in the original paper. For the purpose of this paper the main dimensions were scaled to a length between the perpendiculars of 120 m. The experiments were not performed at the design waterline (DWL) of the vessel, but at a larger draught of 5.28 m, denoted EXPWL in **Figure 1**.

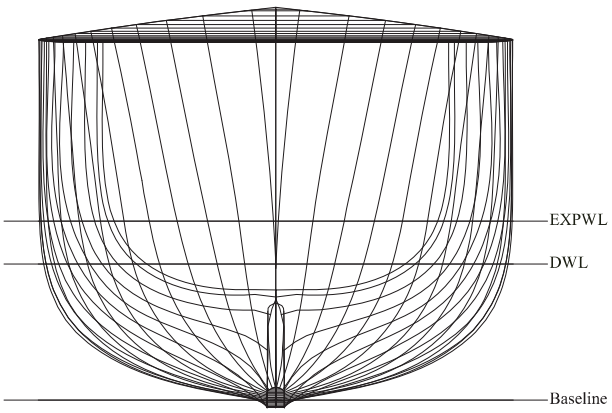

Figure 1 Section plan

Due to the conversion process from a two-dimensional section plan and a lack of longitudinal hull shape information, the displacement and the centre of buoyancy location of the final design differed from the original design. As the intention of the current work was to investigate the behaviour of a generic slender vessel in following waves no further attempt was made to correct the differences in hull parameters.

The propeller and rudder arrangement were not described in the original paper other than the specification of a twin rudder, twin screw arrangement. For this work, a rudder area was chosen of 1% of the lateral area formed by the length between the perpendiculars and the design draught. This is at the lower limit of the usual rudder area for this type of vessel. The propellers were placed at a short distance in front of the rudders, with a diameter of 3.00 meters and a P/D ratio of 1.2.

Table 1 Main particulars

Description	Unit	1982 Value	Current Value
Length between perpendiculars	m	3.660	120.00
Beam	m	0.417	13.67
Draught (EXPWL)	m	0.161	5.28
Draught (DWL)	m	0.122	4.00
Longitudinal centre of buoyancy aft of amidships	m	0.012	6.36[1]
Displacement at EXPWL	kg	127.65	4499054[1]
Radius of gyration about vertical axes	m	0.218 L	0.218 L
Stern arrangement	-	Twin rudder, twin screw	Twin rudder, twin screw
Metacentric height	m	Unknown	1.50
Rudder area	%	Unknown	1%

[1] The center of buoyancy and the displacement given in the original paper were not achievable with the lines provided.

3.2 Numerical modelling details

The forces obtained from the rudders, propellers, and the propeller shafts were determined by using semi-empirical formulations. The rudder formulations accounted for the actual disturbed inflow velocity at the rudder based on the potential flow solution taking into account the orbital velocity from the wave. Rudder emergence was taken into account by determining the wetted span and chord of the rudder below the disturbed water surface and adjusting the forces accordingly. The steering angle was controlled by an autopilot. The settings of the autopilot that were used are given in Table 2.

The propulsion force was determined by the constant rpm setting of the propellers, combined with the inflow velocity at the propeller plane. The rpm setting was determined for the corresponding nominal forward speed in calm water and kept constant during the simulation, The centreline skeg was modelled using combined source and doublet elements combined with a wake sheet extending from its trailing edge. To avoid unrealistic large induced velocities at the hull surface above the skeg, the skeg was extended to the waterline inside the vessel using dummy panels.

Table 2 Auto-pilot settings for course keeping

Description	Symbol	Unit	Value
Damping coefficient	$b_{\delta\psi}$	deg/(deg/s)	9.00
Proportional coefficient	$c_{\delta\psi}$	deg/deg	3.00
Max deflection angle	$\delta_{\max}$	deg	35
Max deflection speed	$\dot{\delta}_{\max}$	deg/s	6.00

Care was taken to ensure fully converged solutions with respect to panel size, time step, wake sheet length, and memory effect length and resolution. Typically around 1300 panels were used on the submerged part of the geometry. The memory effect contributions were truncated at 150 history time steps, and the wake sheet extending from the centre skeg was truncated at 150 panels as well. Time steps

were chosen equivalent to the time necessary to travel 1/50 of the ship length L and kept constant during each simulation.

3.3 Simulation setup

To study the behaviour in following waves, a series of time domain simulations were performed in regular waves. Table 3 presents an overview of the conditions that were simulated. The three different initial headings were tested at the intermediate wave steepness of 1/20 and the three wave steepness were tested at the intermediate initial heading of 20 degrees. This led to a total of 280 individual regular wave time domain simulations of 200 seconds each, requiring about 28 hours in total on a regular desktop computer.

Table 3 Parameter ranges investigated

Description	Parameter	Range	# Variations
Nominal forward speed	Fr	$0.30-0.44$	7
Wave length	λ/L	$0.5-3.0$	8
Wave steepness	H/λ	$1/25, 1/20, 1/17$	3
Initial heading	λ/L	$10°, 20°, 30°$	3

At the start of each simulation the vessel was set to sail at the nominal forward speed with the corresponding rpm setting. The vessel was placed with a wave trough amidships. The wave height and consequently the ship motions were ramped up over 100 time steps. Each time trace was analysed and categorized into one of the following:

- Surf-riding;
- Marginal surf-riding;
- Broaching; or
- None of the above.

The definitions of these characterisations are given in Table 4 and **Table 5**, based on the work of Renilson and Tuite (1998). For the current work no distinction was made between marginal broaching or full broaching, which is the same as the approach taken in an earlier paper (de Jong *et al.*, 2013). The distinction was not found to be very meaningful for this type of simulation and in some cases rather arbitrary.

Table 4 Surf-riding

Description	Surf-riding	Marginal surf-riding
Forward speed	$U = c$	$U \geq 0.9 \cdot c$

Table 5 Broaching (Renilson and Tuite, 1998)

Description	Broach	Marginal broach
Heading deviation	$\psi \geq 20°$	$\psi \geq 20°$
Rudder angle	$\delta = \delta_{max}$	$\delta = \delta_{max}$
Yaw rate	$r > 0$	$r > 0$
Yaw acceleration	$\dot{r} > 0$	-

Prior to the full six degrees of freedom time domain simulations, a number of more basic simulations were carried out. First, a series of calm water runs were performed in order to iteratively determine the calm water trim and sinkage (or rise), as well as the rpm setting necessary for each of the nominal forward speeds. The calm water trim and sinkage were used for determining the mean wetted surface geometry to be used for the linearized radiated and diffracted wave solution.

Second, captive time domain simulations were performed in calm water conditions to capture the manoeuvring coefficients and the steering forces of the vessel and to determine the directional stability over the range of forward speeds of the vessel.

The captive manoeuvring and free running broaching results that are presented in the next section are defined using the axis system given in **Figure 2**. The origin of the ship-fixed frame lies at the centre of gravity of the vessel in the calm water plane. The system is similar to that used for calm water manoeuvring studies. The wave definitions relative to the vessel are used in the free running simulations.

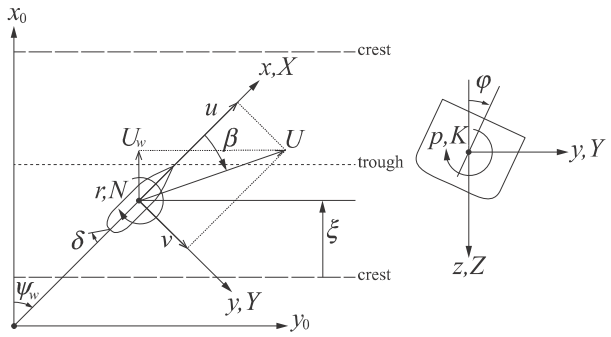

Figure 2 Axis system used for the manoeuvring forces

4. RESULTS

4.1 Manoeuvring

Calm water captive simulations were performed to ensure that the method captured the manoeuvring characteristics of the slender displacement vessel in a realistic manner. The predicted forces and moments in calm water at Froude number 0.40 are compared to those measured by Renilson and Driscoll (1982) at Froude number 0.41 in **Figure 3** to **Figure 6**, and the resulting hydrodynamic coefficients given in **Table 6**.

The dotted blue lines in the figures denote the non-dimensional forces as predicted. The blue solid lines represent the linear component of the fitted polynomial to these forces. The slope of these lines corresponds to the value of the corresponding linear manoeuvring derivative. Deviations between the measured force and the linear fit indicate non-linear contributions to that force component. The slope of green dashed lines represent the value of the calm water manoeuvring coefficients that were reported in the 1982 paper.

The results of the steady drift predictions in Figure 3 and Figure 4 show that both the Y_v and N_v coefficients compare well between prediction and measurement. The results of the yaw oscillations also show a good agreement for N_r in Figure 6. However, the results for the (Y_r-m)-derivative in Figure 5 do not match very well. A possible explanation for this is that this coefficient is the result of the side force distribution over the length of the vessel. For yaw oscillations the contributions to the side force of fore ship and aft ship counteract each other. The difference in their absolute value determines the relatively small magnitude of the resultant side force. The significant mismatch in the longitudinal centre of buoyancy between the original hull and the reconstructed one could cause a relatively large difference, particularly in (Y_r-m).

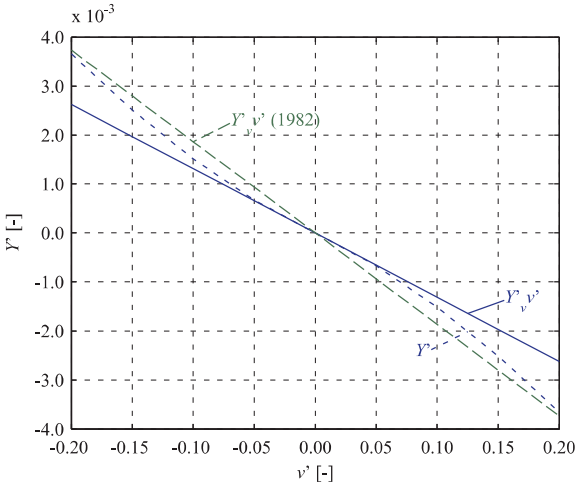

Figure 3 Steady drift: side force computed at three forward speeds and the 1982 measured results

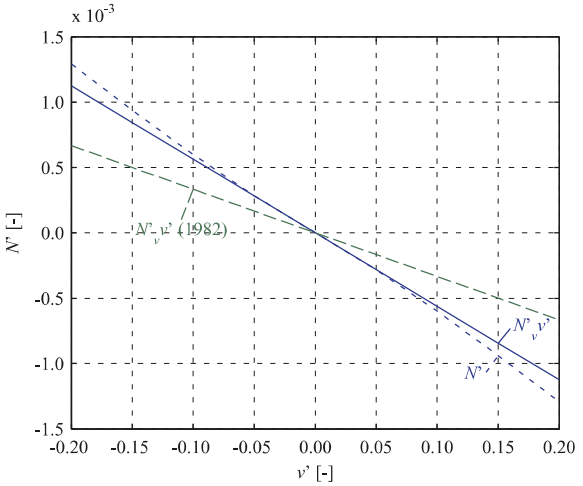

Figure 4 Steady drift: yawing moment computed at three forward speeds and the 1982 measured result

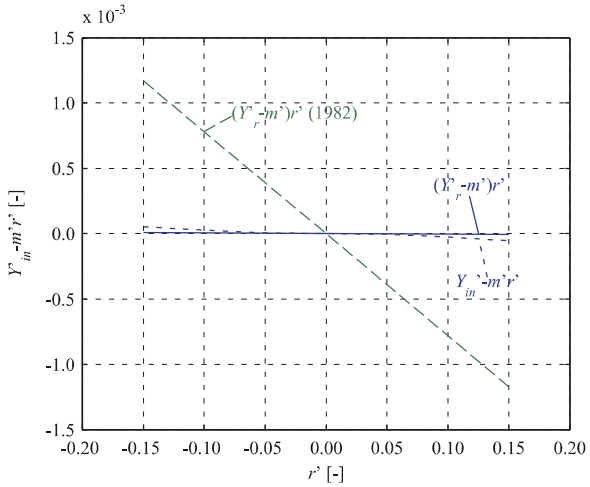

Figure 5 Yaw oscillations: in-phase side force computed at three forward speeds and the 1982 measured results

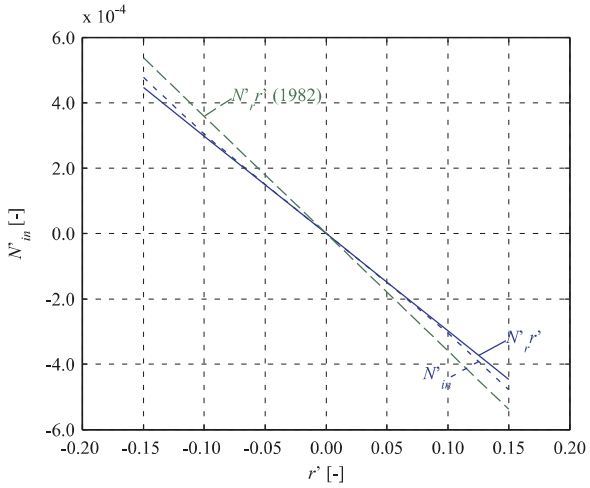

Figure 6 Yaw oscillations: in-phase yawing moment computed at three forward speeds and the 1982 measured results

Table 6 shows the values of the linear manoeuvring coefficients for the 1982 measurement and the current predictions. Also the value of C, given by Eq. (1), is reported.

$$C = Y'_v N'_v - N'_r \left(Y'_r - m' \right) \qquad (1)$$

The quantity C is considered the discriminator for determining whether a ship possesses control-fixed straight-line stability (Lewis, 1989). A positive value for C means, in most cases, that a ship is dynamically stable in the horizontal plane, and will resume on a straight-line path after a disturbance has ended.

Table 6 Results for manoeuvring

	Measured	**Computed**
Fr	**0.412**	**0.400**
Y'_v	-1.87E-02	-1.28E-02
N'_v	-3.33E-03	-5.49E-03
$Y'_r - m'$	-7.81E-03	-5.07E-05
N'_r	-3.59E-03	-2.98E-03
C	+4.09E-05	+3.78E-05

Table 6 indicates that despite the deviation in Y_r'-m', the value of C agrees well between the 1982 measured value and the prediction. The main reason is that the contribution of the first term in Eq. (1) is at least an order of magnitude larger than the contribution of the second term. It can be concluded that both hulls have similar controls-fixed directional stability.

Finally, in **Figure 7** a comparison of the predicted and the 1982 measured steering forces is presented. Although the side force agrees well between computation and measurement, the predicted steering moment was found to be slightly lower than in the 1982 measurements. As the 1982 rudder size could not be recovered, the comparison seems to confirm the chosen relatively small rudder area for the computations. The deviation in steering moment arm can only partly be explained by the deviation in longitudinal centre of buoyancy between original and reconstructed hull.

Although not presented here, turning circle manoeuvres were simulated resulting in predicted turning circles diameters in the order of 4 to 6 times L at full rudder, depending on the nominal forward speed.

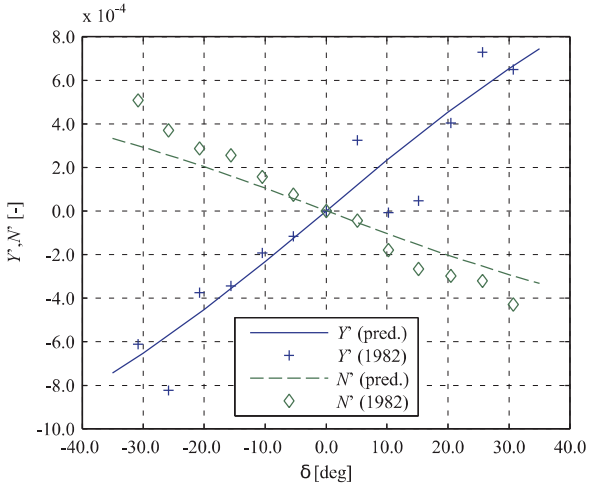

Figure 7 Steering forces: side force and steering moment

4.2 Broaching

The results of the full six degrees of freedom time domain simulations are presented in **Figure 8** to **Figure 13**. First, in **Figure 8** an overview plot is presented for a heading of 20 degrees and wave steepness of 1/20 as an example. Each symbol in the figure represents the outcome of one 200 second time domain simulation. The shape of the symbol indicates categorization of that time trace, using the definitions presented in the previous section.

Furthermore, the figure shows two additional lines. One is marked 'broaching zone' and demarcates the region within which broaches were detected. The other line, marked '$U = c$', indicates the line of zero frequency of encounter, based on the nominal forward speed and wave heading. Below this line, the vessel is initially overtaking the waves, above this line initially the waves are overtaking the vessel.

In both cases the vessel can become entrapped between two wave crests. When the waves are initially overtaking the vessel, this is known as surf-riding. The vessel rides on the front face of the wave, leading to a wave induced moment that tends to force the vessel off course, possibly leading to a broach. The situation where the vessel is initially overtaking the waves has been termed wave-blocking (Maki *et al.*, 2013). In this case the vessel is travelling on the back face of a wave and there is much less risk of upsetting wave forces being built up.

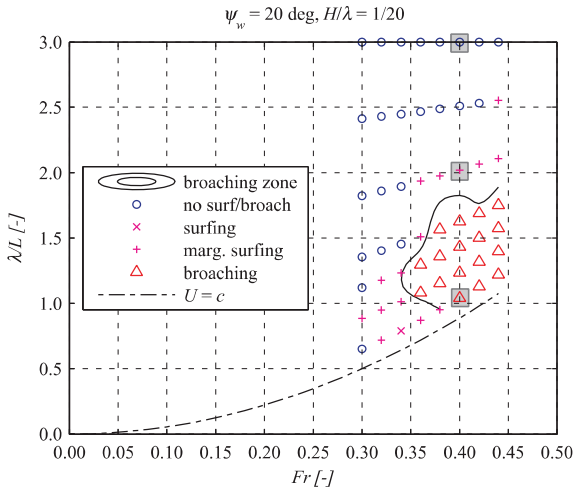

Figure 8 Broaching plot (ψw = 20°, H/λ = 1/20)

Figure 9 to **Figure 11** show relevant time traces of three particular individual time domain simulations performed at Froude number 0.40. The top time trace in each of these figures shows the component of the forward speed of the vessel in the direction of the wave, denoted U_w. The two horizontal red dotted lines mark the wave celerity and 90% of the wave celerity (the threshold for marginal surf-riding). The fourth time trace in each of these figures shows the yaw motion, and the red dotted line indicates a course deviation of 20 degrees (the main threshold value for broaching). The red lines in the last time trace indicate the maximum steering angle. The red circles in the first figure mark the broaches that were detected.

Figure 9 shows the time traces of a run in which broaches were detected. The broaching behaviour is cyclic: within the simulation two broaches occurred. **Figure 10** shows marginal surf-riding, characterised by asymmetric surging with the vessel spending relatively more time close to the wave crest.

Figure 11 shows a situation without surfing or broaching. Although there is still significant

asymmetry in the surge motion, the forward speed in the direction of the wave does not exceed 90% of the wave celerity.

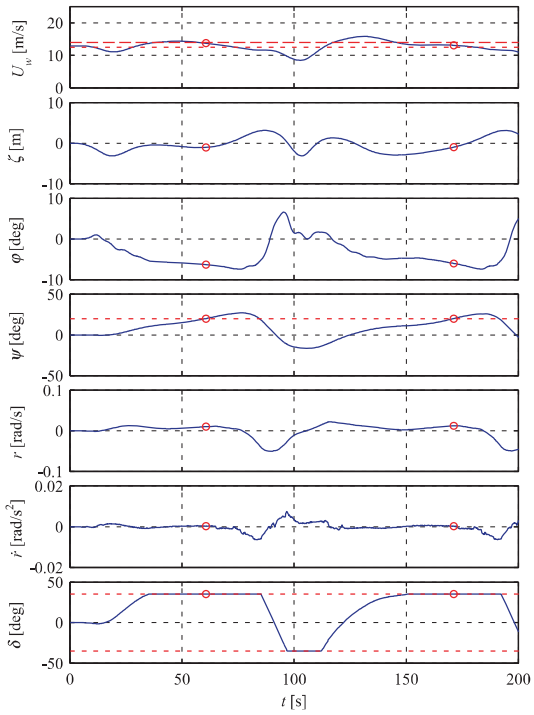

Figure 9 Time traces showing broaching (Fr = 0.40, ψw = 20°, H/λ = 1/20, λ/L = 1.04)

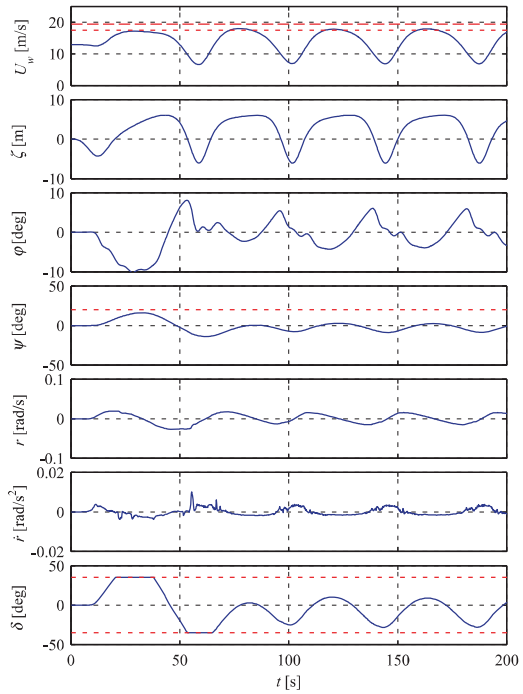

Figure 10 Time traces showing marginal surf-riding (Fr = 0.40, ψw = 20°, H/λ = 1/20, λ/L = 2.02)

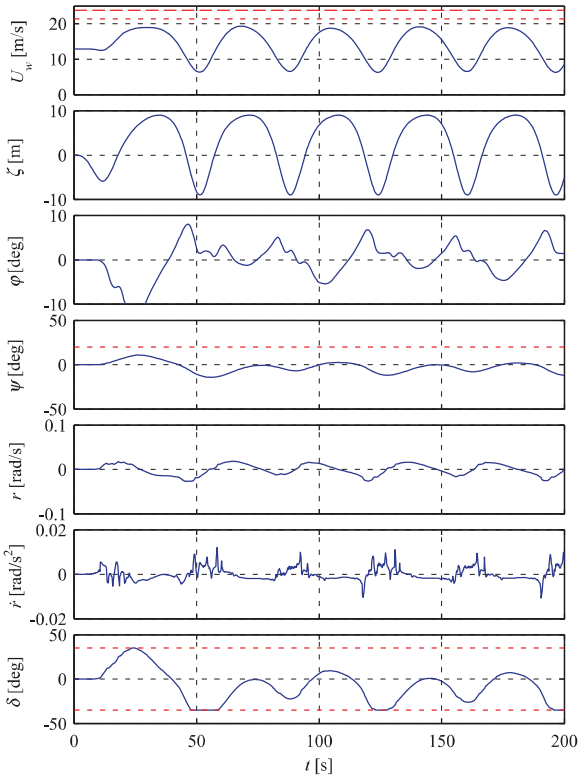

Figure 11 Time traces of no broaching/surf-riding (Fr = 0.40, ψw = 20°, H/λ = 1/20, λ/L = 3.00)

The broaching zones for the variations in initial heading angle are presented in **Figure 12** and the broaching zones for the variations in wave steepness in **Figure 13**. Both figures also show the zero frequency of encounter lines for reference. There is no broaching zone for the smallest heading of 10 degrees in **Figure 12**. For this heading, although surf-riding took place over a significant region, no broaches were detected.

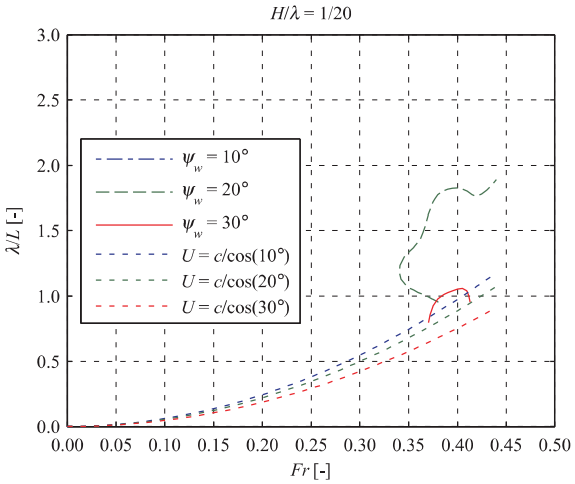

Figure 12 Broaching zones for varying headings

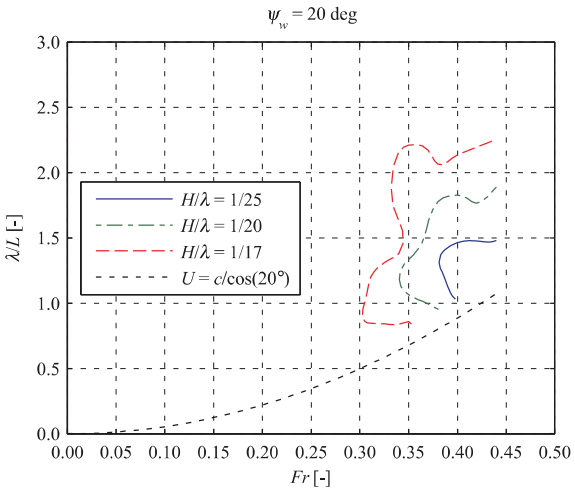

Figure 13 Broaching zones for varying values of the wave steepness

There seems to be a clear progression from no broaching at 10 degrees heading, to a significant broaching region for 20 degrees heading, before diminishing again towards 30 degrees of heading. The fact that the broaching zone is smaller for an initial heading of 30 degrees is counterintuitive, as the wave induced yaw moment at 30 degrees is larger than at 20 degrees. However, this is due to the lower component of the ship velocity in the wave direction when the heading is 30 degrees, resulting in a much lower likelihood of surf-riding.

Figure 13 confirms the expected outcome that the broaching zone expands significantly with increasing wave steepness.

5. DISCUSSION

For a broach to occur there are two conditions to be satisfied: (1) the upsetting wave induced yaw moment should exceed the available restoring steering moment; and (2) this should happen for enough time for the course deviation to build up – hence the link of broaching with surf-riding. The upsetting yaw moment increases with an increasing heading angle, whereas the tendency to surf diminishes with increasing heading angle. This appears to be confirmed by the results presented in this work, showing the largest broaching zone at the intermediate heading.

To compare the results presented in this work with experimental work use was made of results reported by Renilson and Driscoll (1982) and by Nicholson (1974) for similar fine form displacement vessels. Despite differences in hull design and control parameters with these free running experimental investigations, very similar broaching zones were found. The work of Nicholson seems to tend to larger zones at smaller values of the initial heading. Design parameters as metacentric height, rudder size, maximum rudder turning speed and control parameters can have a significant impact on the broaching behaviour and possibly can explain this difference.

De Jong *et al.* (2013) used the same simulation method applied to a water jet powered small rescue craft. Some simulations were carried out at a wave steepness of 1/17 and an initial heading of 20 degrees, allowing a comparison with **Figure 13** in this paper. Although the broaching zones were similar shaped, the rescue craft showed less tendency to broach, with broaching zones starting at slightly larger Froude numbers (0.32 and above) and longer wave lengths (1.1L and above).

Although broaching zones are an useful tool for obtaining a systematic overview of the broaching behaviour of a vessel, and for

comparing the relative performance of alternative designs, the question remains how to use the broaching zone plots for predicting the chance of occurrence and the severity of broaches in realistic irregular seas with directional spreading. Aided by the low frequency of encounter and near quasi-steady behaviour, it might be possible to identify an equivalent regular wave with its own length, height and heading for each passing irregular wave crest and subsequently using the broaching plot to determine the consequences of that wave. The authors are planning to investigate this approach, and compare the results with those obtained in irregular waves, in the future.

6. CONCLUDING REMARKS

Time domain simulations were performed for a fine form displacement vessel with semi-nonlinear panel method with empirical viscous flow corrections. The broaching in regular following to astern quartering waves was simulated to study the effect of: vessel speed; wave length; heading angle to the waves; and wave steepness.

To ensure realistic manoeuvring and course keeping characteristics the results of captive manoeuvring simulations in calm water were compared with earlier experimental data, showing good agreement, despite some differences and unknowns in the design parameters. The deviations found in the side force due to yaw oscillations were shown not to significantly influence the horizontal plane dynamic stability.

The results of time domain simulations were presented as broaching zones, showing the influence of wave heading and wave steepness.

It was found that the broaching zone was larger for a heading of 20 degrees compared to headings of both 10 degrees and 30 degrees. This is due to a greater wave upsetting moment occurring at the greater heading angle, but a lower component of ship speed in the wave direction, and hence less surf-riding at the higher wave heading.

As expected, the tendency to broach was shown to increase with increasing wave steepness.

The broaching zones were found to be similar to zones based on previous free running experimental work with comparable vessels. The question remains how to use these plots for studying the behaviour in realistic irregular seas, and the authors plan to address this in the future.

REFERENCES

Cane, P. du and Goodrich G.J., 1962, "The following sea, broaching and surging", Transactions of the Royal Society of Naval Architects, Vol. 104, pp. 221-228.

Jong, P. de, 2011, "Seakeeping behaviour of high speed ships - An experimental and numerical study", Ph.D. Thesis, Delft University of Technology.

Jong, P. de, Renilson, M.R. and Walree, F. van, 2013, "The broaching of a fast rescue craft in following seas", Proceedings of the 12th International Conference of Fast Sea Transportation, Amsterdam, The Nether-lands.

Lewis, E.V. (ed.), 1989, ""Motions in Waves and Controllability", In Principles of Naval Architecture, Vol. 3, The Society of Naval Architectures and Marine Engineers, NJ, USA.

Maki, A., Umeda, N., Renilson, M.R., and Ueta, T., 2013, "Analytical methods to predict the surf-riding threshold and the wave-blocking threshold in astern seas", Journal of Marine Science and Technology, Vol.19(4), pp. 415-424.

Nicholson, K., 1974, "Some parametric model experiments to investigate broaching-to", International Symposium on the Dynamics

of Marine Vehicles and Structures in Waves, London, UK, pp. 171-177.

Renilson, M.R., 1980, "Broaching in a heavy following sea", The Motor Ship.

Renilson, M.R. and Driscoll, A., 1982, "Broaching – An investigation into the loss of directional stability in severe following seas", Transactions Royal Institution of Naval Architects, Vol. 124, pp. 253-273.

Renilson, M.R. and Tuite, A.J., 1998, "Broaching-to – A proposed definition and analysis method", Proceedings of the 25th American Towing Tank Conference, Iowa, USA.

Walree, F. van, 2002, "Development, Validation and Application of a Time Domain seakeeping method for High Speed Craft with a Ride Control System", Proceedings of the 24th Symposium on Naval Hydrodynamics, Fukuoka, Japan, pp. 475-490.